Overview of Terrain Relative Navigation Approaches for Precise Lunar Landing

Andrew E. Johnson and James F. Montgomery
aej@jpl.nasa.gov, monty@jpl.nasa.gov
Jet Propulsion Laboratory, California Institute of Technology
Pasadena, CA 91109

Abstract—The driving precision landing requirement for the Autonomous Landing and Hazard Avoidance Technology project is to autonomously land within 100m of a predetermined location on the lunar surface. Traditional lunar landing approaches based on inertial sensing do not have the navigational precision to meet this requirement. The purpose of Terrain Relative Navigation (TRN) is to augment inertial navigation by providing position or bearing measurements relative to known surface landmarks. From these measurements, the navigational precision can be reduced to a level that meets the 100m requirement.

There are three different TRN functions: global position estimation, local position estimation and velocity estimation. These functions can be achieved with active range sensing or passive imaging. This paper gives a survey of many TRN approaches and then presents some high fidelity simulation results for contour matching and area correlation approaches to TRN using active sensors. Since TRN requires an a-priori reference map, the paper concludes by describing past and future lunar imaging and digital elevation map data sets available for this purpose.

TABLE OF CONTENTS

1. INTRODUCTION

Hazard Detection and Avoidance (HDA) and Terrain Relative Navigation (TRN) are onboard capabilities that combine sensing and computing to achieve autonomous safe and precise landing. The Autonomous Landing and Hazard Avoidance Technology (ALHAT) project is developing HDA and TRN capabilities for lunar landing. The driving precision landing requirement for the ALHAT system is to autonomously land within 100m of a predetermined location on the lunar surface. Traditional lunar landing approaches based on inertial sensing do not have the navigational precision to meet this requirement. The purpose of TRN is to augment inertial navigation by providing position or bearing measurements relative to known surface landmarks. From these measurements, the navigational precision can be reduced to a level that meets the 100m requirement.

As shown in Figure 1, there are three different TRN functions: global position estimation, local position estimation and velocity estimation. These functions can be achieved with active range sensing or passive imaging.

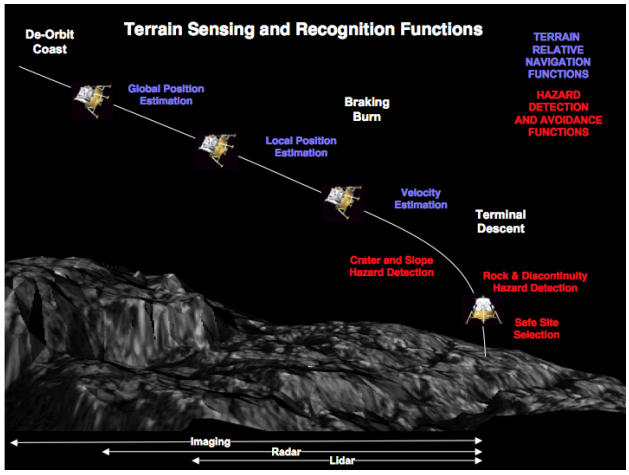

Figure 1: Terrain sensing and recognition functions for safe and precise lunar landing.

Initial work in the Terrain Relative Navigation area focused on conducting a survey of existing TRN approaches. The results of this survey are given in Section 2. . To determine where on the lunar surface TRN is possible, Section 3. describes the availability of lunar reference maps for TRN. Based on the TRN survey and the

1-4244-1488-1/08/$25.00 ©2008 IEEE.
IEEEAC paper #1657, Version 2, Updated December 14th, 2008

requirement to land anywhere on the surface of the moon under any lighting conditions, it appears that active ranging correlation approaches to TRN are very promising. To further refine the understanding of these approaches, simulations of their performance have been conducted for various lunar terrain types. The results of these simulations are given in Section 4. .

2. SURVEY OF TRN APPROACHES

To assist in the development of the ALHAT GNC Guidance Navigation and Control (GN&C) architecture for lunar landing, the different approaches to TRN have been compared and contrasted in a survey of TRN approaches. This survey will feed into system level trades that will determine the TRN approaches that ALHAT pursues for development. Ten different approaches are presented in Table 1.

The approaches can be split into two categories based on the type of sensor supplying the terrain data: passive imaging or active range sensing. Passive imaging has the advantage that the sensors (visible cameras) are mature and easy to accommodate on the lander (i.e., low power, mass and volume). Some of the passive imaging approaches can provide navigation measurements from any altitude. However passive imagers have the distinct disadvantage that they cannot operate in the dark; they require solar illumination or an illumination source on the lander. The high altitude for TRN operation makes the illumination source approach impractical and requiring solar illumination places excessive constraints on landing time of day. The active range sensing approaches have the advantage that they operate under any illumination conditions. However, space qualified active range sensors are less mature than passive imagers and they have a limited maximum operating range which places constraints on the altitude at which TRN measurements can be made available.

The approaches can be further broken down into two categories based on the navigation information provided by the approach: *global position estimation* and *local position estimation*. Global position estimation provides absolute measurement of lander position with respect to a global coordinate system attached to a surface map that has been constructed from orbital reconnaissance acquired before landing. The desired landing site is specified within this *global map*, so positions estimates with respect to this map can be used to guide the lander to the desired landing site. Global position estimation is used during descent to achieve the 100m global landing precision.

In contrast, the approaches for local position estimation provide position estimates with respect to a map of the landing site made by onboard sensors during landing. This *local map* is typically at a higher resolution than the global map, so the local position estimates are more precise than the global ones. This added precision makes these approaches useful when guiding the lander to safe landing site away from landing hazards. However, the local position estimates cannot be used to improve absolute position because they do not involve direct comparisons to the global reference map.

In local position estimation, a local map is constructed and then subsequent surface measurements are compared back to this map. This persistent comparison back to the same map prevents the growth of errors in the local position estimate. However, when the difference in resolution between the local map and the surface measurements becomes too large, a new local map must be generated. If the local map changes every time a surface measurement is taken then local position estimation is essentially estimating surface relative velocity. *Velocity estimation* is a less accurate subset of local position estimation because the velocity errors are integrated when generating a position estimate. However, velocity estimation may be desirable because it is simpler to implement and the errors measurements are independent whereas persistent comparisons back to the same map may produce correlated errors in position.

The TRN approaches can also be broken down based on the structure of the algorithm used to compare surface measurements to the map. In *correlation* approaches, a contiguous patch of the surface is acquired using the onboard sensor. If a passive imager is used, then the patch is essentially a subset of the image; for a range sensor, the patch is elevation map or contour. This patch is then correlated, in the image processing sense, with the onboard map. Correlation algorithms place the patch at every location in the map and then measure the similarity between the patch and the map values (This process can be visualized as raster scanning the patch across the map.) If the values are similar, then the location is given a high score; if they are not similar, then the location is given a low score. The location in the map with the highest score is chosen as the best match location for the patch in the map. Interpolation of the correlation scores is used to obtain a sub-pixel estimate of the match position. The orientation (and altitude for imagers) is then used to compute the position of the lander in the map coordinate system.

P*attern matching* approaches use landmark matching instead of patch correlation. Landmarks are locations that can be extracted reliably from map and surface data and also have distinct characteristics (i.e., the pattern) that make them amenable to comparison to other landmarks. For example, craters are often used as landmarks because they can be extracted reliably from image data over a broad range of image scales and illuminations and the diameter of the crater is an identifier that can be used for matching. The relative distances and angles between landmarks are also used during the matching procedure.

Pattern matching algorithms share the following typical process. The map is preprocessed to detect landmarks and these landmark locations and distinct characteristics are

stored in a database. The surface data is acquired and the same process is applied to detect landmarks. The characteristics (e.g., crater diameters) of the surface data landmarks and the map landmarks are then compared. If the characteristics between two landmarks are similar, then the landmarks are hypothesized to match. Note that this comparison of characteristics is in contrast to correlation approaches where the surface data and map are compared directly to each other. The next step is to take groups of matching landmarks and confirm that the distance and angles between landmarks in the map are the same as those in the surface data. If they are, then the set of landmark matches is geometrically consistent and the position (and possibly orientation) of the lander can be computed by aligning the position of the landmarks in the map with the position of the landmarks in the surface data.

Correlation is a common 2D signal processing operation, so very fast implementations are possible using FPGA or DSP chips. Correlation approaches have the additional advantage that they do not require the existence of distinct landmarks near the landing site. However they are typically more sensitive to differences between the map and surface data than pattern matching approaches. They also have the disadvantage that the surface data must be rectified (i.e., orientation and possibly scale and perspective differences removed) to the local level coordinate frame of the map so that correlation can be applied. This causes a coupling between errors in the position estimate derived from correlation and the attitude (and possibly altitude) estimate use to reorient the surface data. Pattern matching does not require rectification, so this coupling is not present.

Table 1 compares and contrasts ten different approaches to TRN. The purpose of each column in the tables is described below:

- Sensor Modality: passive imaging or active range sensing.
- Function: Position estimation function provided by approach (Global or local)
- Sensor: Sensor used to acquire surface data
- Approach: A description of the approach that includes whether the approach uses pattern matching or correlation
- Required Inputs: The input measurements and map information needed by the algorithm to produce the output
- Output Estimate: The estimate(s) generated by the algorithm
- Strengths: Qualitative assessment of the strength of each approach relative to the other approaches.
- Limitations: Qualitative assessment of the weaknesses of limitations of each approach relative to the other approaches
- Significant Non-Space Applications: If they exist, significant non-space applications are listed because they can possibly be redesigned for the lunar application. Or at the very least be used as design examples to reduce the development cost and risk of the proposed approach.

Since the descriptions in the tables are rather terse, the algorithm for each approach is described briefly below by approach ID.

1. Crater Pattern Matching for Position Estimation [5][6][22] - This is a pattern matching approach to global position estimation using passive visible imagery. Craters are detected in a map of the landing site and stored in a database. During landing, craters are detected in descent imagery and are matched to the craters in the database. This approach to position estimation has been tested with imagery from the Moon, Mars and asteroids. Using data from the Near Earth Asteroid Rendezvous mission, it has been shown to produce position estimation results that are as accurate as those derived from manual crater identification methods. This approach could also be used for local position estimation by detecting and tracking crater(s) through multiple descent images.
2. Scale Invariant Feature Transform (SIFT) [2][14] - This pattern matching approach is the same as the crater approach above except that it uses a different landmark representation called SIFT developed by David Lowe at University of British Columbia. The SIFT landmarks are very general in that they can be extracted from imagery that do not have craters. This generality comes at the cost of some sensitivity to illumination and viewing angle.
3. Onboard Image Reconstruction for Optical Navigation (OBIRON) [9][10] - OBIRON is a hybrid pattern matching and correlation approach developed for small body navigation. It uses prior reconnaissance imagery to build 3D models of surface patches. These patches become the landmarks used for navigation. During landing, the 3D patches are rendered using the current solar illumination to create landmark images. These landmarks are then correlated with images taken during decent to estimate offsets from the current estimate of lander position and attitude. OBIRON is a general landmark approach that has been tested off-line with imagery from the NEAR and MUSES-C asteroid missions.
4. Image to Map Correlation for Position Estimation [4][17][21] - This correlation approach compares a descent image directly to an orbital image of the landing site. First the descent image is rectified to the same scale and orientation as the map and a patch of the image is correlated with the map. This approach has been used terrestrially to guide cruise missiles (DSMAC). Development and testing of an approach tailored to lunar and Mars landing has been developed at JPL. This approach has been tested with imagery from the Moon and other solar system bodies. It has also been successfully tested with imagery and inertial

Table 1: Survey of Terrain Relative Navigation Approaches

ID	Sensing Modality	Function	Sensor	Approach	Required Inputs	Output Estimate	Strengths	Limitations	Significant Non-Space Application
1	Passive Visible	Position Estimation	Camera	Crater Pattern Matching for Position Estimation	descent image; crater landmark database	absolute position (and attitude)	insensitive to changes in illumination; does not require attitude or altitude measurements	requires solar illumination; requires cratered terrain	
2				Scale Invariant Feature Transform (SIFT) Pattern Matching for Position Estimation	descent image; SIFT landmark database	absolute position (and attitude)	general representation should work for all terrains including ones without craters; does not require attitude or altitude measurements	requires solar illumination; illumination changes between image and map are not well tolerated; large out-of-plane rotations degrade performance	Terrestrial rover navigation
3				Onboard Image Reconstruction for Optical Navigation (OBIRON) - Surface Patch Correlation for Position Estimation	multiple overlapping orbital images to construct map; descent image; lander attitude; lander altitude	absolute position (and attitude update)	general representation should work for all terrains including ones without craters; built in accommodation of illumination changes and terrain relief	requires solar illumination; requires multiple overlapping images of landing site; requires rendering of landing site map prior to landing; requires attitude and altitude estimate	
4				Image to Map Correlation for Position Estimation	map image; descent image; lander attitude; lander altitude	absolute horizontal position	general representation should work for all terrains including ones without craters; requires just one orbital image and no 3D modeling for rerendering	requires solar illumination; possibly sensitive to large illumination changes and terrain relief	Raytheon Cruise Missile DSMACS. Original is TRL 9. Currently being upgraded
5		Velocity Estimation	Camera	Descent Image Motion Estimation Subsystem (DIMES) - Consecutive Image Correlation for Velocity Estimation	3 descent images; 3 attitude estimates, 3 altitude estimates	average horizontal velocity	general representation should work for all terrains	requires solar illumination, need overlap between consecutive images	
6				Structure From Motion - Consecutive Image Correlation for Velocity and Attitude Rate Estimation	2 descent images; 2 altitudes	average velocity (and angular rate) between images	does not require attitude estimate, general representation should work for all terrains; fast implementation and very accurate	requires solar illumination; need overlap between consecutive images	
7	Active Range Sensing	Position Estimation	Imaging LIDAR	Shape Signature Pattern Matching for Position Estimation	range image; motion correction data; shape signature data based from 3D map	absolute position (and attitude)	general approach solves for position and attitude without prior knowledge of these measurements; independent of lighting conditions;	long processing time; more general than needed; requires significant terrain relief; LIDAR is less mature than camera	Object Recognition from Range Data
8				Range Image to DEM Correlation for Position Estimation	range image or scans; motion correction data; absolute attitude estimate; digital elevation map	absolute position	independent of lighting conditions; more robust than Altimeter to DEM correlation	Requires scanner , gimbal or imaging array; LIDAR is less mature than camera.	
9			Altimeter	Altimeter to DEM Correlation for Position Estimation	altimetry swath; motion correction data; absolute attitude estimate; digital elevation map	absolute position	independent of lighting conditions; sensors likely to work at higher altitude possibly up to 100km	requires long contour; LIDAR is less mature than camera.	Raytheon Cruise Missile TERCOM Original is TRL 9. Currently being upgraded
10		Velocity Estimation	Imaging LIDAR	Consecutive Range Image Correlation for Velocity Estimation	2 range images; motion correction data; 2 attitudes	average horizontal and vertical velocity	independent of lighting conditions;	need image overlap;	

measurements from a sounding rocket test flight.

5. Descent Image Motion Estimation Subsystem (DIMES) [16]- The DIMES algorithm correlates image patches from one descent image to the next to estimate velocity of a lander. Before tracking each descent image is rectified to the local level frame using on-board estimates of position and altitude. DIMES was tested extensively in the field and performed successfully for both Mars Exploration Rover landings. DIMES can be extended to estimate local position.
6. Structure From Motion [3][20]- In Structure from Motion multiple image patches are correlated from descent image to descent image. From these tracks the motion of the lander and the range to the patches is computed up to an unknown scale factor. When given an altitude measurement, the output is an estimate of change in position and attitude between images. No rectification is required for correlation if the images are acquired fast enough. Structure from motion has been tested extensively using terrestrial imagery and has been

ported to an autonomous helicopter testbed where it has been used to estimate motion during autonomous landing.

7. Shape Signature Pattern Matching [8][13]– Shape signatures are surface landmarks based on local surface shape that can be used for a pattern matching approach to TRN. A digital elevation map (DEM) of the landing site is processed to extract the signatures. During landing, range images are acquired and from them signatures are extracted. The signatures are then matched between DEM and range image and a position and attitude estimate are computed. Spin-images[13] have been tested with terrestrial images of desert terrain.
8. Range Image to DEM Correlation [1]- In range image to DEM correlation, a digital elevation map is constructed from a single or multiple range images acquired during descent. The onboard attitude estimate is used rotate the range measurements into the map frame for elevation map construction. This Descent DEM is then correlated with the Global DEM provided by orbital sensors to obtain a position fix. This approach has been tested using simulated lunar imagery.
9. Altimeter to DEM Correlation [11]- Altimeter to DEM correlation is similar to the approach above except that the Descent DEM is reduced to a single column that is populated with elevation data by an altimeter. This approach has been used to guide terrestrial cruise missiles (TERCOM) and for the lunar application it has been tested with simulated altimetry.
10. Consecutive Range Image Correlation [1][14][18]- Correlation of consecutive range images [14] takes two range images and rotates them into the map local level frame using the onboard attitude estimate. The two maps are then correlated with each other to determine a change in position. This approach has been tested with terrestrial ranges images and implemented on a space qualified microprocessor (RAD 3000). A variant of this approach that reduces the sensitivity to an initial motion estimate [18] uses a programmable scan pattern to image local surface patches. The motion estimate is then derived from the change in range of multiple surface patches.

3. LUNAR REFERENCE MAPS FOR TRN

Absolute position estimation requires a reference map. This can only be performed where such maps exist, and the position estimate can only be as precise as the resolution of the reference map. The highest resolution existing Lunar maps with global coverage are:

- Imagery: Global 100m/pixel from Clementine UVVIS imager. Significant gaps including regions at the poles.
- DEM (Digital Elevation Map): Global 7.6 km/pixel (at the equator) from Clementine laser altimeter. No polar coverage above 82˚ and below -79˚ latitude.

Images with higher resolution were taken by the Clementine, Apollo, Lunar Orbiter and Ranger missions, but only for small portions of the moon. Based solely on existing map resolution, the best possible landing precision with near global coverage would be 100m and TRN would be limited to visible imaging approaches; matching to a 7.6 km resolution DEM is not viable for TRN. Furthermore, these approaches would be restricted to higher altitudes (> 5km) due to the large difference in pixel sizes between the preexisting map and descent images acquired at low altitudes. Better landing precision is possible if the landing sites are restricted to the areas imaged at higher resolution by previous missions, but these sites may not fit with future exploration plans.

The Lunar Reconnaissance Orbiter (LRO) is a lunar orbiter scheduled for launch in 2008 [7]. LRO has two instruments that will provide reference map data useful for TRN: the LRO Camera (LROC) and the Lunar Orbiter Laser Altimeter (LOLA). LRO is tailored to polar reconnaissance. Above 86˚ north and south latitude LRO will provide:

- Imagery from LROC: 0.5m/pixel total coverage
- DEM from LOLA: 25m-35m/pixel with sub meter vertical precision and total coverage

These polar maps have enough resolution to achieve the 100m landing precision requirement for both passive visible and active ranging approaches to TRN.

The anticipated LRO DEM coverage is sparsest at the equator. There is a longitudinal separation of 1.1 km between LOLA swaths and LROC will only be able to image selected areas at 0.5m/pixel (LROC will image the entire moon at 100m/pixel with its wide area camera). With expected post-processing, this translates into global DEM coverage of 1 km per pixel, which is slightly better than that available from previous missions. However, LRO will image 50 selected sites at a much higher resolution. At these 50 sites the maps are expected to be:

- Imagery from LROC: 1m/pixel mosaics over 100 square kilometers
- DEM from multiple view LROC stereo: 1-2m/pixel over 25 square kilometers

Within these sites and their associated area, both passive visible and active ranging approaches to TRN will have maps of high enough resolution to achieve the 100m landing precision requirement. If more area is needed for TRN to achieve position fixes earlier on in the trajectory, it would be desirable to align multiple high resolution landing areas at key locations to better support a single landing area.

4. ANALYSIS OF LIDAR-BASED TRN

ALHAT is developing a precision landing system that must work under any lighting conditions. Since passive imaging approaches require solar illumination, they cannot meet this requirement. As described in the section above, digital elevation maps (DEM) of the lunar surface will exist

after the successful completion of the LRO mapping mission. Pattern matching approaches using surface or shape data exist, but they are computationally inefficient when compared to correlation approaches. All of these factors indicate that active ranging correlation approaches are attractive for lunar TRN.

Simulation Components

A simulation of active ranging correlation has been developed to refine our understanding of these approaches and possibly set requirements on applicable precision navigation sensors. The simulation consists of:

Synthetic terrain maps developed under ALHAT that that have slope and crater distributions that match lunar terrain types. Hutton and Evensen classified the lunar surface into four terrain types: smooth mare, rough mare, hummocky uplands and rough uplands [12]. Each terrain type has a crater distribution model that described crater probability versus diameter per unit area. They also described mean lunar slope as a function of slope baseline for the four terrain types. Synthetic terrains were generated that matched the models for the four terrain types. Examples of these terrain maps are given in Figure 2.

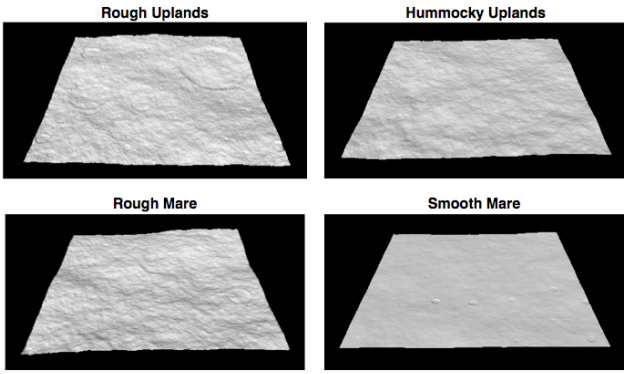

Figure 2: Synthetic lunar terrain maps for each lunar terrain type.

A LIDAR simulator has been developed under the Mars program at JPL. This simulator is described in detail elsewhere [15]. Essentially, it simulates a scanning LIDAR in motion above a surface represented by a digital terrain map. For each laser pulse, the ranging model simulates that intersection of the pulse with the terrain (by modeling the pulse as multiple rays emanating from the sensor) and applies representative return detection logic to simulate the range measurement performance (c.f., Figure 3). Applying this ranging model over a field of regard generates scans or range images. The scanning pattern is parameterized so that arbitrary fields of view and resolutions can be generated. The synthetic terrain and the trajectory describing the motion are read from a file, so they can be provided from an arbitrary source.

An algorithm for correlating range images or altimeter swaths to a DEM has been developed using components of DIMES [16] and range image correlation for velocity estimation [14]. The algorithm takes as input a reference elevation map that contains the region of the lunar surface below the lander when TRN is performed; this region does not necessarily include the landing site if TRN is used sufficiently far down-range, but it must be large enough to cover the landing dispersions. The active ranging sensor collects some range data and the algorithm uses estimates of lander attitude and motion during data collection to place the range data in a local level coordinate frame that is parallel to the reference map. When sufficient data has been collected, a sensor elevation map is constructed by gridding the range data. This sensor elevation map is then correlated with the reference elevation map. If the correlation peak is sufficiently high, narrow and higher than other secondary peaks, then a correlation is considered valid. For each valid correlation, the absolute global position of the lander can be computed from the location of the correlation peak. A block diagram of the algorithm is given in Figure 4.

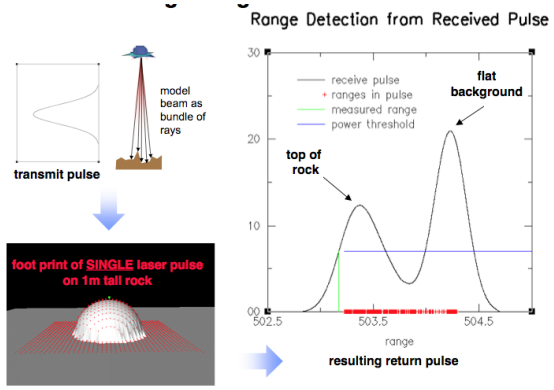

Figure 3: Ranging model used in LIDAR simulator.

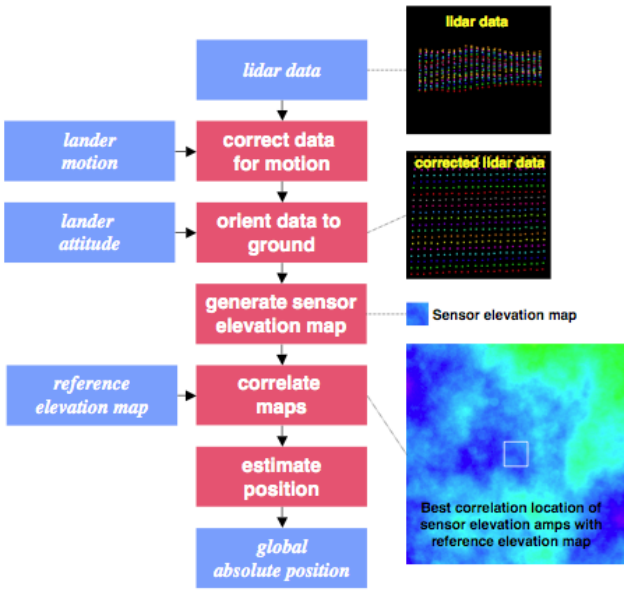

Figure 4: Active ranging TRN algorithm block diagram.

Analysis Results

This simulation has been used to assess, in a Monte Carlo sense, the performance of two correlation approaches to active ranging TRN: Altimeter to DEM correlation (TRN approach #9 in Section 2.) and range image to DEM correlation (TRN approach #8 in Section 2.). Each approach was simulated over the four lunar terrain types described above. The simulation generated multiple Monte Carlo test cases by shifting the lander trajectory with respect to the synthetic terrain maps used to generate the range data. This forces the LIDAR data and resulting sensor elevation map to be different for each test case. For each test case, LIDAR data is simulated and the algorithm is executed. If a valid correlation is reported then the global position estimate is compared to the true global position and a position error is computed. This procedure is repeated for multiple test cases (lander positions with respect to the reference map) and statistics of percent valid correlations and mean and standard deviation of position error are generated. This Monte Carlo simulation is performed with different trajectory parameters, lunar terrain types and algorithm parameters to investigate the sensitivity of the approach.

Altimeter to DEM correlation is an attractive approach to TRN because altimeters do not require a scanner and can operate from high altitude. The parameters investigated by Monte Carlo simulation for this approach are (c.f., Figure 5): operating altitude, the down track extent of the altimeter swath used for correlation and the resolution of the reference elevation map used for correlation. The simulation uses a trajectory provided members of the ALHAT Team at Johnson Space Center to generate the down track motion and altitude. The LIDAR simulator parameters are set such that at the given altitude, the beam width is equal to the map resolution (e.g., at 10000m altitude, with a 10m map resolution, the beam width is 1 mrad). The LIDAR simulator parameters are also set such that on average one altitude measurement is made for every map resolution size step down track (e.g., if the vehicle is moving at 1600m/s and the map resolution is 40m then altitude measurements are taken at 40 Hz). Setting the parameters in this way enforces one altitude measurement per map pixel and a total sampling of the contour to prevent aliasing effects during correlation due to subsampling of the contour. Finally, the range detection mode in the LIDAR simulator is set to the mean of the return pulse (instead of leading edge) because this will be closer to the average over the map pixel elevation provided by a DEM.

The results of the simulation for Smooth Mare terrain are given in Figure 6 (surprisingly, the results for the other terrain types were comparable to Lunar Smooth Mare, so they are not shown). The tables describe the TRN performance with two metrics. The 95% CEP (Circular Error Probable) metric is the circular error radius in meters that contains 95% of the position errors; this metric indicates that accuracy of the approach with respect to the parameters. If this number is much larger than the map resolution then more than 5% of the test cases resulted in an incorrect match. The Valid Correlation Fraction metric describes the fraction (0.0 to 1.0) of test cases that were marked as valid after the correlation checks described above were applied; this metric indicates the reliability of the position estimate.

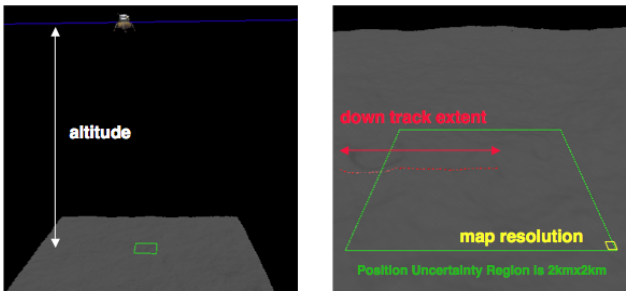

Figure 5: Parameters investigated in Altimeter to DEM Correlation simulation.

Altimeter to DEM Correlation
10 m Map Resolution

down track extent (m)	altitude (m) 2500	5000	10000	20000	
200	1047.86	1038.52	1063.61	1122.56	95% CEP (m)
	0.04	0.04	0.04	0.01	Valid Correlation Fraction
400	20.98	19.04	19.09	17.74	95% CEP (m)
	0.52	0.49	0.44	0.34	Valid Correlation Fraction
800	17.40	19.36	18.61	16.06	95% CEP (m)
	0.86	0.82	0.81	0.81	Valid Correlation Fraction
1600	19.31	19.21	16.36	15.91	95% CEP (m)
	0.91	0.89	0.89	0.89	Valid Correlation Fraction

Altimeter to DEM Correlation
40 m Map Resolution

down track extent (m)	altitude (m) 2500	5000	10000	20000	
200	1252.14	1241.43	1206.02	1206.15	95% CEP (m)
	0.02	0.03	0.02	0.03	Valid Correlation Fraction
400	1188.35	1185.86	1167.00	1146.12	95% CEP (m)
	0.03	0.03	0.03	0.03	Valid Correlation Fraction
800	937.22	1034.98	941.79	906.75	95% CEP (m)
	0.16	0.17	0.17	0.16	Valid Correlation Fraction
1600	80.77	80.28	82.01	77.67	95% CEP (m)
	0.58	0.60	0.62	0.60	Valid Correlation Fraction

Figure 6: Simulation results for Lunar Smooth Mare terrain and Altimeter to DEM Correlation TRN

As the simulation results show, map resolution and down track extent have a strong effect on performance while altitude has little effect. Altitude has little effect because the LIDAR simulator parameters were changed at each altitude as described above which by matching altimeter beam width and rate to map resolution essentially eliminated the effect of altitude. Although this is not easy to do in flight with LIDAR hardware, it does indicate the best possible performance for TRN at a specific altitude.

For maps with 10m pixels, the down track swath must be at least 1600m to achieve a CEP on order of the map

resolution and a Valid Correlation Fraction near 90%. These results are encouraging because they indicate that it is possible to correlate a single swath of altimetry with lunar terrain and obtain accurate and reliable position estimates. For 40m maps, as expected the performance is worse. It is not until the down track extent reaches 1600m that accurate position estimates are generated and even then, the number of valid matches is relatively low when compared to the results with 10m maps. With both map resolutions the 1600m down track results have a 95% CEP which is on order twice the map resolution.

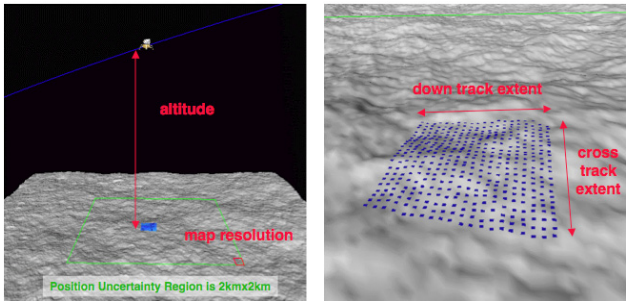

Figure 7: Parameters investigated in Range Image to DEM Correlation.

Range image to DEM correlation might have some advantages over altimeter to DEM correlation because an area instead of a contour is correlated. These advantages include more accurate and robust position estimates because an area with more elevation values instead of a contour is correlated and less time to acquire data because a long contour collected over time is not required. The down side of this approach is that it needs a way to split or scan the beam, which is not required for altimetry.

To investigate this approach, the altimetry simulation was augmented with a 1D scanner that scanned perpendicular to the down track direction. As the lander travels across the lunar surface multiple 1D scans are taken in a push broom fashion. These scans cover an area instead of a contour. The parameters investigated by Monte Carlo simulation for this approach are (c.f., Figure 7) operating altitude, the down track extent of the scans, the cross track extent of each scan and the resolution of the reference elevation map used for correlation. The JSC trajectory was used to provide sensor motion, and the LIDAR parameters were set to match beam width to map resolution as described above for altimetry to DEM correlation. In addition, the LIDAR field of view was set to obtain the specified cross track extent at the specified altitude (e.g., at 2500m altitude with a 200m cross track width, the FOV was set to 2*atan((200/2)/2500) = 4.6˚). The sample rate was set so that on average one LIDAR sample was taken in each map pixel size area in both the cross track and down track directions (e.g., for a 200 m/s horizontal velocity, a 200 m cross track width, a 400 m down track width, and 10m pixels, the LIDAR sample rate was set to (200m/s / 400m) * (400m / 10m/pix) * (200m / 10m/pix) = 400pix/s = 400Hz). As described above, the range detection mode in the LIDAR simulator was set to the mean of the return pulse.

The results of the simulation for Smooth Mare terrain are given in Figure 8 (As before, the results for the other terrain types were comparable to Lunar Smooth Mare, so they are not shown). As was the case with altimeter to DEM correlation, altitude has little effect on the results because the LIDAR parameters were set for each altitude to match the sampling to the map resolution.

Map resolution and the size of the area scanned have a strong effect on the results. For 10m maps, the results have a high valid fraction and a CEP that is less than 10m for all cross track and down track widths. This indicates that 10m maps will generate reliable and accurate position estimates for range images down to 200m x 200m.

For 40m maps, range images with areas around 800m x 800m are needed to obtain valid fractions near 90% and CEP less than the 40m map resolution. These areas are rather large but not unexpected. With a 40m map resolution, 800m x 800m maps have 20x20 pixels which is the same number of pixels as the 200m x 200m results for 10m maps. A tentative conclusion from this is that 20x20 pixels are required to obtain accurate and reliable position estimates.

For both 10m and 40m maps, the 95% CEP for range image to DEM correlation is around one half the map resolution. This is on average four times more accurate than the altimeter to DEM correlation results for more the same map resolution. Furthermore, only 200 to 800 meters of down track travel is required to for range image to DEM correlation while altimeter to DEM correlation requires at least 1600m of down track travel. The conclusion is that range image correlation is more accurate and can generate measurements at a faster rate than altimeter correlation. Of course this improved performance comes at the cost of requiring at least a 1D imaging/scanning capability on the LIDAR.

5. Conclusion

There exist multiple viable approaches to terrain relative navigation for precise lunar landing. Passive visible cameras have the advantage of high resolution reference maps and low cost sensors while active ranging approaches can operate under any lighting condition which lifts restrictions on landing time of day and allows for landing in permanently dark craters. New simulation results indicate that LIDAR-based TRN is robust and highly accurate.

Acknowledgment

The work described in this publication was performed at the Jet Propulsion Laboratory, California Institute of Technology, under contract from the National Aeronautics and Space Administration. The authors would like to thank

Tye Brady at the Charles Stark Draper Laboratory for participatin in the assessment of the use of LRO data for TRN and Ron Sostaric at the Johnson Space center for providing the lunar descent trajectory used in the simulations.

Range Image to DEM Correlation

10 m map resolution, 2500 m altitude

down track extent (m)	cross track extent (m) 200	400	800	
200	5.21	5.02	4.98	95% CEP (m)
	0.93	0.98	0.97	Valid Fraction
400	4.82	4.03	4.30	95% CEP (m)
	0.98	1.00	1.00	Valid Fraction
800	4.62	4.30	4.15	95% CEP (m)
	0.99	1.00	1.00	Valid Fraction

Range Image to DEM Correlation

10 m map resolution, 5000 m altitude

down track extent (m)	cross track extent (m) 400	800	1600	
400	4.49	4.44	4.38	95% CEP (m)
	1.00	1.00	1.00	Valid Fraction
800	4.40	4.33	4.18	95% CEP (m)
	1.00	1.00	1.00	Valid Fraction
1600	4.27	4.23	4.15	95% CEP (m)
	1.00	1.00	1.00	Valid Fraction

Range Image to DEM Correlation

40 m map resolution, 2500 m altitude

down track extent (m)	cross track extent (m) 200	400	800	
200	1079.50	66.09	28.49	95% CEP (m)
	0.03	0.15	0.38	Valid Fraction
400	432.18	29.05	20.25	95% CEP (m)
	0.11	0.31	0.58	Valid Fraction
800	29.89	25.18	18.83	95% CEP (m)
	0.32	0.63	0.89	Valid Fraction

Range Image to DEM Correlation

40 m map resolution, 5000 m altitude

down track extent (m)	cross track extent (m) 400	800	1600	
400	29.61	20.59	19.35	95% CEP (m)
	0.31	0.58	0.84	Valid Fraction
800	22.90	19.00	18.99	95% CEP (m)
	0.58	0.87	0.98	Valid Fraction
1600	21.65	19.13	17.15	95% CEP (m)
	0.62	0.95	1.00	Valid Fraction

Figure 8: Simulation results for Lunar Smooth Mare terrain and Range Image to DEM CorrelationTRN.

REFERENCES

[1] J. Aggarwal and B. Sabata, "Estimation of Motion from a Pair of Range Images: A Review," *Computer Vision, Graphics, and Image Processing*, **54**(3), pp. 309-324, 1991.

[2] A. Ansar, "2004 small body GN&C research report: Feature recognition algorithms," in *Small Body Guidance Navigation and Control FY 2004 RTD Annual Report (Internal Document)*. Pasadena, CA: Jet Propulsion Laboratory, , no. D-30282 / D-30714, pp. 151–171, 2004.

[3] J.-Y. Bouguet and P. Perona, "Visual Navigation Using a Single Camera," *Proc. IEEE Int'l Conf. Computer Vision*, (ICCV), 1995

[4] J.C. Carr and J. L. Sobek, "Digital Scene Matching Area Correlator (DSMAC)," *Image Processing for Missile Guidance, Proceedings of the Society of Photo-Optical Instrumentation Engineers*, **238**, pp. 36-41, 1980.

[5] Y. Cheng, A. Johnson, C. Olson, and L. Matthies, "Optical landmark detection for spacecraft navigation," *Proc. 13th Annual AAS/AIAA Space Flight Mechanics Meeting*, 2003.

[6] Y. Cheng and A. Ansar, "Landmark based Position Estimation for Pinpoint Landing on Mars," in *Proc. IEEE Int'l Conf. on Robotics and Automation (ICRA)*, pp. 4470–4475, 2005,.

[7] G. Chin et al., "Lunar Reconnaissance Orbiter Overview: The Instrument Suite and Mission," *Space Science Reviews*, **129**(4), pp. 391-419, 2007.

[8] A. Frome and D. Huber and R. Kolluri and T. Bulow and J. Malik, "Recognizing Objects in Range Data Using Regional Point Descriptors," *Proc. European Conf. on Computer Vision (ECCV)*, 2004.

[9] R. Gaskell, "Automated Landmark Identification for Spacecraft Navigation," *Proc. AAS/AIAA Astrodynamics Specialists Conf.,* AAS Paper # 01-422, 2001.

[10] R. Gaskell "Determination of Landmark Topography from Imaging Data," *Proc. AAS/AIAA Astrodynamics Specialists Conf.*, Paper # AAS 02-021, 2002.

[11] J. P. Golden, "Terrain Contour Matching (TERCOM): a Cruise Missile Guidance Aid," *Image Processing for Missile Guidance, Proc. Soc. Photo-Opt. Instr. Eng.,* **238**, pp. 10-18, 1980.

[12] R. Hutton and D. Evensen, "Lunar Surface Models,' TRW Internal Report for NASA, May 5th, 1972.

[13] A. Johnson and M. Hebert. "Using Spin Images for efficient multiple model recognition in cluttered 3-D scenes." IEEE Transactions on Pattern Analysis and Machine Intelligence, **21**(5), pp. 433-449, 1999.

[14] A. Johnson and M. SanMartin, "Motion Estimation from Laser Ranging for Autonomous Comet Landing," *Proc. Int'l Conf. Robotics and Automation* (ICRA '00), pp. 132-138, 2000.

[15] A. Johnson, A. Klumpp, J. Collier and A. Wolf, "Lidar-based Hazard Avoidance for Safe Landing on Mars," *AIAA Journal of Guidance, Control and Dynamics*, **25**(5), October 2002.

[16] A. Johnson, R. Willson, Y. Cheng, J. Goguen, C. Leger, M. SanMartin and L. Matthies, "Design Through Operation of an Image-Based Velocity Estimation System for Mars Landing," *International Journal of Computer Vision*, **74**(3), pp. 319-41, 2006.

[17] A. Johnson, A. Ansar, L. Matthies, N. Trawny, A.I. Mourikis, and S.I. Roumeliotis, "A General Approach to Terrain Relative Navigation for Planetary Landing", *Proc. 2007 AIAA Infotech at Aerospace Conference*, May 7-10.

[18] J. de LaFontaine, D. Neveu and J-F. Hamel, "Psuedo Doppler Velocity Navigation for Lidar-based Planetary Exploration*," Proc. AAS/AIAA Astrodynamics Specialists Conf.,* Paper # AIAA 2006-6664, 2006.

[19] D. G. Lowe, "Distinctive image features from scale-invariant keypoints," *International Journal of Computer Vision*, **60**(2), pp. 91–110, 2004.

[20] J. Montgomery, A. Johnson, S. Roumeliotis and L. Matthies, "The JPL Autonomous Helicopter Testbed: A Platform for Planetary Exploration Technology Research and Development*," Jour. Field Robotics; Special Issue on UAV's*, **23**(3), 2006.

[21] Y. Sheikh, S. Khan, M. Shah and R. Cannata, "Geodetic Alignment of Aerial Video Frames," Chapter in *Video Registration* Eds: Mubarak Shah and Rakesh Kumar, Kluwer Academic Publishers, 2003

[22] Wetzler, P. G., Honda, R., Enke, B., Merline, W. J., Chapman, C. R., and Burl, M. C, "Learning to Detect Small Impact Craters," *Proc. 7th IEEE Wrksp. on Application of Computer Vision*, 2005.

BIOGRAPHIES

Dr. Andrew Johnson *is a Principal Member of Technical Staff in the Computer Vision Group at JPL. He is the terrain sensing algorithm lead for the Autonomus Landing and Hazard Avoidance Project which is developing technology for safe and precise landing for the next generation manned lunar lander. At JPL he works on development, validation and flight implementation of computer vision systems for planetary landers and Mars rovers. He was the lead algorithm developer for the Mars Exploration Rover Descent Image Motion Estimation System and is currently developing the rover Visual Odometry algorithm from the Mars Science Laboratory.*

Dr. James Montgomery *is a Senior Member of Technical Staff at the Jet Propulsion Laboratory and is a member of the Guidance Navigation and Control Section. He has more than 15 years of experience in mobile robotics research and development and over 20 years of experience in software systems development for engineering applications, primarily in the fields of real-time embedded control, and signal and image processing. Since joining JPL, he has led the design, development and field testing of the JPL Autonomous Helicopter Testbed. He has also been involved in numerous technology development tasks for ground and aerial robots as well as planetary landing systems. He is currently the GN&C/EDL Field Test Lead for the Mars Science Laboratory Project.*